Mon. Not. R. Astron. Soc. **000**, 000–000 (0000) Printed 15 February 2007 (MN LATEX style file v2.2)

Dispersion Measure Variations and their Effect on Precision Pulsar Timing

X. P. You,[1,2,3⋆] G. Hobbs,[2] W. A. Coles,[4,2] R. N. Manchester,[2] R. Edwards,[2] M. Bailes,[5] J. Sarkissian,[2] J. P. W. Verbiest,[5,2] W. van Straten,[6] A. Hotan,[7] S. Ord,[8] F. Jenet,[6] N. D. R. Bhat,[5] A. Teoh[5,2]

[1] *National Astronomical Observatories, Chinese Academy of Sciences, Beijing 100012, China*
[2] *Australia Telescope National Facility, CSIRO, PO Box 76, Epping, NSW 1710, Australia*
[3] *Graduate University of Chinese Academy of Sciences, Beijing 100049, China*
[4] *Electrical and Computer Engineering, University of California at San Diego, La Jolla, California, USA*
[5] *Centre for Astrophysics and Supercomputing, Swinburne University of Technology, P. O. Box 218, Hawthorn VIC 3122, Australia*
[6] *Center for Gravitational Wave Astronomy, University of Texas at Brownsville, TX 78520*
[7] *School of Mathematics and Physics, University of Tasmania, Hobart TAS 7001, Australia*
[8] *School of Physics, University of Sydney, NSW 2006, Australia*

ABSTRACT

We present an analysis of the variations seen in the dispersion measures (DMs) of 20 millisecond pulsars observed as part of the Parkes Pulsar Timing Array project. We carry out a statistically rigorous structure function analysis for each pulsar and show that the variations seen for most pulsars are consistent with those expected for an interstellar medium characterised by a Kolmogorov turbulence spectrum. The structure functions for PSRs J1045−4509 and J1909−3744 provide the first clear evidence for a large inner scale, possibly due to ion-neutral damping. We also show the effect of the solar wind on the DMs and show that the simple models presently implemented into pulsar timing packages cannot reliably correct for this effect. For the first time we clearly show how DM variations affect pulsar timing residuals and how they can be corrected in order to obtain the highest possible timing precision. Even with our presently limited data span, the residuals (and all parameters derived from the timing) for six of our pulsars have been significantly improved by correcting for the DM variations.

Key words: pulsars: general — ISM: general

1 INTRODUCTION

The Parkes Pulsar Timing Array (PPTA) is a project which aims to take advantage of the extraordinary rotational stability of short period (millisecond) radio pulsars. The principal goal of the PPTA is to make a direct detection of gravitational waves (Hobbs 2005; Manchester 2006). For this purpose it is necessary to measure weekly times of arrival (TOAs) of ∼20 pulsars with a precision between 100 and 500 ns (Jenet et al. 2005). In order to achieve this goal all systematic errors in the TOAs must be considered and, if possible, corrected. One such correction is the delay caused by the plasma between the pulsar and the Earth. Most of this plasma contribution is from the interstellar medium, but the contribution of the solar wind cannot be neglected and the ionosphere will occasionally be important. The dispersion in the plasma is a linear effect and can, in principle be corrected exactly. The group delay, $t_g(\nu)$, is related to the integral of the electron density, n_e, from the Earth to the pulsar, $t_g(\nu) = \mathrm{DM}/(K\nu^2)$, where

$$\mathrm{DM} = \int_0^L n_e \, \mathrm{d}l, \tag{1}$$

is the "dispersion measure". The dispersion constant $K \equiv 2.410 \times 10^{-4}\,\mathrm{MHz^{-2}\,cm^{-3}\,pc\,s^{-1}}$, ν is the observing frequency and L the distance from the Earth to the pulsar. When TOAs, t_{g1} and t_{g2}, are measured at two frequencies, ν_1 and ν_2, the DM can be estimated using

$$\mathrm{DM} = K\frac{t_{g2} - t_{g1}}{\nu_2^{-2} - \nu_1^{-2}}. \tag{2}$$

A rough estimate of the DM of a (radio) pulsar is generally obtained from the discovery observations. This estimate can be quickly refined by re-observing the pulsar with more widely separated frequencies. Measured DMs for currently

⋆ Email: xpyou@bao.ac.cn

known radio pulsars lie between 2.38 and 1235 cm^{-3} pc and from 2.65 to 244 cm^{-3} pc for the subset of millisecond pulsars (Manchester et al. 2005)[1].

Precise measurements of DM show that it often has significant time variations. A time delay of 100 ns at an observing frequency of 1400 MHz, the accuracy goal of the PPTA, corresponds to a DM variation of 4.72×10^{-5} cm^{-3} pc. Variations of this order can occur in the ionosphere only for zenith angles in excess of 80° or during major geomagnetic storms, so ionospheric corrections will not normally be necessary. At this level of timing precision, significant variations in DM can occur due to the solar wind even when the pulsar is 60° away from the Sun. Variations in the interstellar plasma DM result from plasma turbulence and usually have a Kolmogorov power spectrum, implying that the variations are larger over longer time-scales. In the pulsars observed by the PPTA project, such DM fluctuations can reach levels that require correction within a few days or weeks.

It is clear that the goals of the PPTA project cannot be reached without measuring the DM and correcting for the plasma delay for each observation. The most precise TOA measurements are usually obtained at a frequency of 1400 MHz, but the only dual-band receiver available at the Parkes telescope is at 685 and 3100 MHz. Thus the DM variations are measured using the dual-band system at different times than the TOA observations at 1400 MHz. Since the DM varies relatively smoothly, the DM correction can be interpolated to the epoch of the primary TOA observation. In this paper we use the first few years of DM measurements to test methods of correcting for the solar wind, to study the interstellar plasma turbulence and to derive algorithms for correcting the TOA measurements.

2 CAUSES OF DM VARIATIONS

The contributions of the ionosphere and the solar wind have been well-studied and can be estimated by various methods independently of the PPTA. The total electron content of the ionosphere ("TEC") is regularly monitored because it is needed to correct the Global Positioning System (GPS) navigational system. A monitor is located at the Parkes observatory, but it is seldom necessary to make this correction. Corrections for the solar wind are implemented in the standard pulsar timing codes TEMPO and TEMPO2 (Hobbs et al. 2006; Edwards et al. 2006). However, these assume a spherically symmetric solar wind with a constant scale factor and do not model observed variations in wind density with latitude, longitude and time which can be as much as a factor of four at any distance (McComas et al. 2000). The earlier package, TEMPO, assumes a higher density compared to TEMPO2. Neither of these is adequate for the desired PPTA precision.

The DM due to the interstellar medium varies for a variety of reasons. For example, variations are known to occur for some pulsars within supernova remnants, when wisps of ionised gas drift across the line of sight to the pulsar. For instance, the DM of the Vela pulsar decreased at a rate of 0.04 $\mathrm{cm}^{-3}\,\mathrm{pc\,yr}^{-1}$ from 1970 to 1985 (Hamilton et al. 1985). Similarly the Crab pulsar shows variations up to 0.02 $\mathrm{cm}^{-3}\,\mathrm{pc\,yr}^{-1}$ over 15 yr (Lyne et al. 1988). Pulsars in binary systems which exhibit eclipses show DM variations from the ionised envelope of the companion object. These have been measured for two of the binary pulsars in the globular cluster 47 Tucanae (Freire et al. 2003). The DM change of 0.0065 cm^{-3} pc for one of these, PSR J0023−7203J, is 100 times the level that would require correction for the PPTA pulsars. Even larger changes have been observed in PSR B1259−63 which is in orbit with a massive B2e star, reaching 10.7 and 7.7 cm^{-3} pc during the periastron passages of 1994 and 1997, respectively (Wang et al. 2004).

The DM also varies due to turbulent spatial variations which drift across the line of sight between the Earth and the pulsar. These have commonly been characterised in the literature as linear slopes in DM. Measurements of such $\mathrm{dDM/d}t$ values for four pulsars were discussed by Backer et al. (1993) who proposed that $\mathrm{dDM/d}t \propto (\mathrm{DM})^{1/2}$ and modelled the variation using wedges of enhanced density. Observations of 374 pulsars were presented by Hobbs et al. (2004) who found the same relationship. However, a better characterisation of the DM variations can be made using the theoretical spatial characteristics of a turbulent process. As shown later, in a turbulent model the relation $\mathrm{dDM/d}t \propto (\mathrm{DM})^{1/2}$ arises naturally and does not require a wedge model. The spatial power spectrum of electron density was defined by Rickett (1990) as

$$P(q) = C_n^2 q^{-\beta}; \qquad 2\pi/l_o < q < 2\pi/l_i, \tag{3}$$

where C_n^2 scales the power spectrum (and thus the total energy in the process), β is the power-law exponent (which is 11/3 for a Kolmogorov spectrum), l_o is the outer scale and l_i is the inner scale. Physically the outer scale is identified with the largest scale in the medium, typically the size at which it becomes inhomogeneous, and the inner scale is the scale at which dissipation occurs. Energy is introduced at some scale between l_o and l_i, supporting the spectrum. This energy 'cascades' in frequency to l_i where it is dissipated. Turbulent variations in electron density can be estimated from DM variations and various diffractive phenomena such as angular scattering, pulse broadening and intensity scintillations. Diffractive variations are caused by much smaller scale fluctuations in density and thus probe different regions of the spatial spectrum than DM variations. Diffractive variations are modulated by refractive variations which can be used to probe scales between the diffractive and the DM scales. All these observed variations result from the motion of the line of sight through the scattering medium, thus spatial variations of scale s are associated with temporal variations of scale T by $s = VT$ where V is the velocity of the line of sight with respect to the scattering plasma. Therefore, the inner time-scale τ_i corresponds to $l_i = V\tau_i$.

Radio scattering observations, such as those mentioned above, are directly sensitive to a statistic called the "phase structure function", $D_\phi(\tau)$, which is defined by

$$D_\phi(\tau) = \langle[\phi(t+\tau) - \phi(t)]^2\rangle, \tag{4}$$

where ϕ is the geometrical phase delay between the source and the observer and the angle brackets denote an ensemble average. For a power-law spatial spectrum with $2 < \beta < 4$ between the inner and outer scales, the structure function

[1] http://www.atnf.csiro.au/research/pulsar/psrcat

D_ϕ is given by (Rickett 1977):

$$D_\phi(\tau) = (\tau/\tau_d)^\alpha\,, \tag{5}$$

where $\alpha = \beta - 2$. Similarly, we can define a structure function for the DM variations:

$$D_{\rm DM}(\tau) = \langle[{\rm DM}(t+\tau) - {\rm DM}(t)]^2\rangle. \tag{6}$$

At scales that are larger than the scale of refractive scintillation, the geometrical phase approaches the actual phase (Coles et al. 1991) and these two structure functions can be related through the dispersion relation (Equation 2),

$$D_{\rm DM}(\tau) = (K\nu/2\pi)^2\, D_\phi(\tau). \tag{7}$$

The structure function was first used to investigate DM variations by Rickett (1988). Subsequently, the technique was applied to PSR J1939+2134 (B1937+21) by Cordes et al. (1990), Kaspi et al. (1994) and Ramachandran et al. (2006). Cordes et al. (1990) showed that the structure function was consistent with a power-law fluctuation spectrum with index β between 11/3, the Kolmogorov value, and 4. Kaspi et al. (1994) continued this work and obtained $\beta = 3.874 \pm 0.011$. From the approximate agreement of the diffractive timescale τ_d computed from Equation 5 and the directly measured value, Cordes et al. (1990) inferred that the inner scale of the fluctuation spectrum, l_i, was less than about 2×10^7 m. Recently, Ramachandran et al. (2006) extended the data-span to 20 yr and obtained $\beta = 3.66 \pm 0.04$ which is consistent with the value expected for a Kolmogorov spectrum and suggested $l_i \sim 1.3 \times 10^9$ m. Cognard & Lestrade (1997) presented the DM variations of a different millisecond pulsar, PSR J1824−2452 (B1821−24), and obtained $\beta = 3.7 \pm 0.2$ which is also consistent with a Kolmogorov spectrum. Dispersion measure variations were measured for six pulsars by Phillips & Wolszczan (1991) and structure functions were obtained for PSRs B0834+06, B0823+26 and B0919+06. Measured power-law indices were in the range 3.77 to 3.87 with uncertainties of 0.04 or less.

Assuming that the DM variations are due to turbulence then, from the definition of the structure function, the "slope" d${\rm DM}/{\rm d}t$, averaged over an interval τ, will be a random variable with an rms of $[D_{\rm DM}(\tau)]^{1/2}/\tau$. This can be related to the mean DM value by the distance to the pulsar L as both DM and $D_{\rm DM}(\tau)$ are proportional to L. Thus the observed result that ${\rm d}{\rm DM}/{\rm d}t \propto ({\rm DM})^{1/2}$ is expected for any turbulent medium and does not require ad hoc models such as the wedge model of Backer et al. (1993). This proportionality will be valid for spatial scales $V\tau$ that are less than the parsec scale of interstellar clouds, since it assumes that contributions to the DM fluctuations from various points on the line of sight add incoherently.

There have been three dissipation mechanisms discussed in the literature: ion cyclotron damping (which is the primary mechanism in the solar wind), Landau damping and ion-neutral collisional damping. It is not thought that Landau damping is important in the ISM (Minter & Spangler 1997). Ion cyclotron damping will certainly occur if the turbulent cascade reaches the small spatial scales involved. It occurs at the ion inertial scale (Coles & Harmon 1989),

$$L_i = 684\,{\rm km}/\sqrt{n_e({\rm cm}^{-3})} \tag{8}$$

and has been clearly observed in the solar wind. Expected scales in the ISM range from 300 to 3000 km and it has almost certainly been observed at scales of 300 to 800 km using pulse broadening observations (Bhat et al. 2004). Damping due to ion-neutral collisions is also a resonant process that occurs near the ion-neutral collision frequency and would result in scales of ∼30 AU in typical warm ISM conditions (Minter & Spangler 1997).

3 OBSERVATIONS AND DATA ANALYSIS

The PPTA, which commenced observations in February 2004, uses the Parkes 64-m radio telescope to make timing observations of 20 millisecond pulsars. One, PSR J1824−2452, lies within the globular cluster M28, the others within the disk of our Galaxy. Table 1 lists basic parameters for the 20 PPTA pulsars: J2000 name, period (P), period derivative ($\dot{P}$), orbital period (P_b) if the pulsar is in a binary system, DM, distance based on the NE2001 electron density model (Cordes & Lazio 2002) unless the annual parallax or another independent distance estimate is available, total proper motion (μ) and ecliptic latitude (b_E). Because PSRs J1022+1001 and J1730−2304 lie very close to the ecliptic plane, timing methods cannot provide a precise proper motion in ecliptic latitude; for these two pulsars the proper motion in ecliptic longitude is given. Each pulsar is typically observed at intervals of 2–3 weeks at frequencies close to 685 MHz (50 cm), 1400 MHz (20 cm) and 3100 MHz (10 cm), where the band designations (based on wavelength) are given in parentheses. We have used three backend systems: a wideband correlator (WBC), a digital filterbank system (DFB1)[2] and the Caltech-Parkes-Swinburne Recorder 2 (CPSR2), a coherent dedispersing system, all of which record orthogonal linear polarisations. The WBC provides 2-bit sampling with a bandwidth of up to 1024 MHz for the earlier data. The DFB1 was installed in 2005 June and allows 8-bit sampling of a 256 MHz bandwidth at 10 cm and 20 cm. Observations at 10 and 50 cm are obtained simultaneously using a dual-band receiver providing bandwidths of 64 MHz at 50 cm and 1024 MHz at 10 cm. Most observations at 20 cm are made using the central beam of the Parkes multibeam receiver although the "H-OH" receiver has occasionally been used for observations in this band. Data are simultaneously recorded using the CPSR2 baseband recording system with 2-bit sampling of two 64-MHz bands, centred on 1341 and 1405 MHz respectively, and either the WBC or DFB1 with 256 MHz bandwidth. At 50 cm, data are recorded using one band of CPSR2. For all receivers, a linearly polarised broadband calibration signal can be injected into the feed at 45° to the two signal probes.

Observation times per pulsar are typically either 32 min or 64 min and data are folded on-line with sub-integration times of 1 min for the WBC and DFB1 and 16 s for CPSR2. All pulsar observations are preceded by a short (2 min) observation of a pulsed calibration signal. For most pulsars the WBC and DFB1 data are split into 512 frequency channels with between 256 and 1024 phase bins across the pulse period. For CPSR2, the data are coherently dedispersed in each of 128 frequency channels with 1024 phase

[2] A new digital filterbank system (DFB2) with a wider bandwidth and improved resolution is currently under construction.

Table 1. Parameters for the PPTA pulsars.

PSR	P (ms)	$\dot{P}$ (10^{-20})	P_b (d)	DM ($\mathrm{cm^{-3}pc}$)	Dist. (kpc)	μ (mas $\mathrm{yr^{-1}}$)	b_E (°)
J0437−4715	5.757	5.73	5.74	2.6	0.16[a]	140.89	−67.87
J0613−0200	3.062	0.96	1.20	38.8	1.71	7.3	−25.41
J0711−6830	5.491	1.49	...	18.4	0.86	21.9	−82.89
J1022+1001	16.453	4.33	7.81	10.3	0.30[a]	17	−0.064
J1024−0719	5.162	1.85	...	6.5	0.39	81	−16.04
J1045−4509	7.474	1.77	4.08	58.1	1.96	7.8	−47.71
J1600−3053	3.598	0.95	14.35	52.3	1.63	4.1	−10.07
J1603−7202	14.842	1.56	6.31	38.1	1.17	8.5	−49.96
J1643−1224	4.622	1.85	147.02	62.4	2.41	9	9.78
J1713+0747	4.570	0.85	67.83	16.0	1.12[a]	6.4	30.70
J1730−2304	8.123	2.02	...	9.6	0.53	20.5	0.19
J1732−5049	5.313	1.38	5.26	56.8	1.41[a]	—	−27.49
J1744−1134	4.075	0.89	...	3.1	0.36	20.99	11.81
J1824−2452	3.054	162.00	...	119.9	3.09	4.7	−1.55
J1857+0943	5.362	1.78	12.33	13.3	0.91[a]	6.16	32.32
J1909−3744	2.947	1.40	1.53	10.4	1.14[a]	36.99	−15.16
J1939+2134	1.558	10.50	...	71.0	3.57	0.80	42.30
J2124−3358	4.931	2.05	...	4.6	0.27	49.0	−17.82
J2129−5721	3.726	2.07	6.63	31.9	1.36	8	−39.90
J2145−0750	16.052	2.98	6.84	9.0	0.50[a]	14.1	5.31

[a] Distance obtained from a parallax measurement.

bins. Off-line processing uses the PSRCHIVE software system (Hotan et al. 2004). For all recording systems, data from frequency channels or sub-integrations which are obviously affected by radio-frequency interference are excised, as are channels from the outer edges of the band (typically about 5 per cent of the band at each edge) where the system gain is low. Data are then calibrated for variations of instrumental gain and phase across the band using observations of the pulsed calibration signal and the Stokes parameters formed.

For all pulsars except PSR J0437−4715, pulse TOAs were obtained by cross-correlating a template profile with the Stokes I mean pulse profile for each observation. For most of the observed pulsars, errors in the calibration procedure resulted in TOA errors which were less than the uncertainty due to random (receiver) noise. However for PSR J0437−4715 at 20 cm and 50 cm, this was not the case and it was advantageous to use the polarimetric invariant interval instead of Stokes I (Britton et al. 2000). Template profiles were formed for each instrument and each observing frequency (685, 1341, 1405 MHz for CPSR2, 1369 and 3100 MHz for the DFB1, 1433 and 3100 MHz for the WBC) by weighted summing of all available data to form 'grand average' profiles and then blanking the baseline regions. Figure 1 shows the grand average Stokes I profiles at the three frequencies for all 20 pulsars (except for PSR J2129−5721 where we have data for two frequencies only).

For DM measurements, profile alignment across frequencies is an important issue. The template profiles for a given pulsar were approximately aligned using the cross-correlation of each profile with a reference profile. However, because of frequency-dependent profile variations, there remains some uncertainty in the true alignment. In this work, we are primarily concerned with variations in DM, not absolute values, so arbitrary phase offsets between data obtained using different systems were included in the timing model.

The resulting TOAs were analysed using TEMPO2. Timing model parameters were obtained by fitting standard pulsar timing parameters (including astrometric, spin and binary parameters) to the 20 cm and/or the 10 cm observations[3]. As we are interested in DM variations, we do not fit for any time derivatives of the DM as part of the timing model; however, we do allow TEMPO2 to model the DM variations due to the solar wind (this is further discussed in §5.2). The timing model parameters were subsequently held constant in order to obtain timing residuals at all observing frequencies.

To obtain the time variations in DM, $\Delta\mathrm{DM}(t)$, we fitted Equation 2 to segments of timing data. The segment lengths were adjusted so that each segment contained at least one observation at each frequency (typically 1 or 2 weeks). Initially we used the 10 and 50 cm observations to obtain $\Delta\mathrm{DM}(t)$ because these were obtained simultaneously and are well separated in frequency. However, if the pulse profile at 10 cm or 50 cm has a low signal-to-noise ratio, we also used 20 and 50 cm or 10 and 20 cm to obtain $\Delta\mathrm{DM}(t)$.

The structure function is a useful statistic for studying the physical process causing the DM variations. Calculation of the structure function is straightforward, even for unequally-spaced data (Equation 6). However, the estimation of the errors in the structure function due to uncertainties in the $\Delta\mathrm{DM}(t)$ values, and due to the finite duration of the $\Delta\mathrm{DM}(t)$ series has not been discussed consistently in the literature. Because of the irregular data-sampling, τ represents a "bin" with a width which we have adjusted to give

[3] We use residuals obtained using CPSR2, WBC and DFB1. However, for a few pulsars with high DM and short period, the WBC profile is significantly smeared and therefore, for PSRs J0613−0200, J1600−3053, J1824−2452, J1939+2134, we only use the CPSR2 and DFB1 observations.

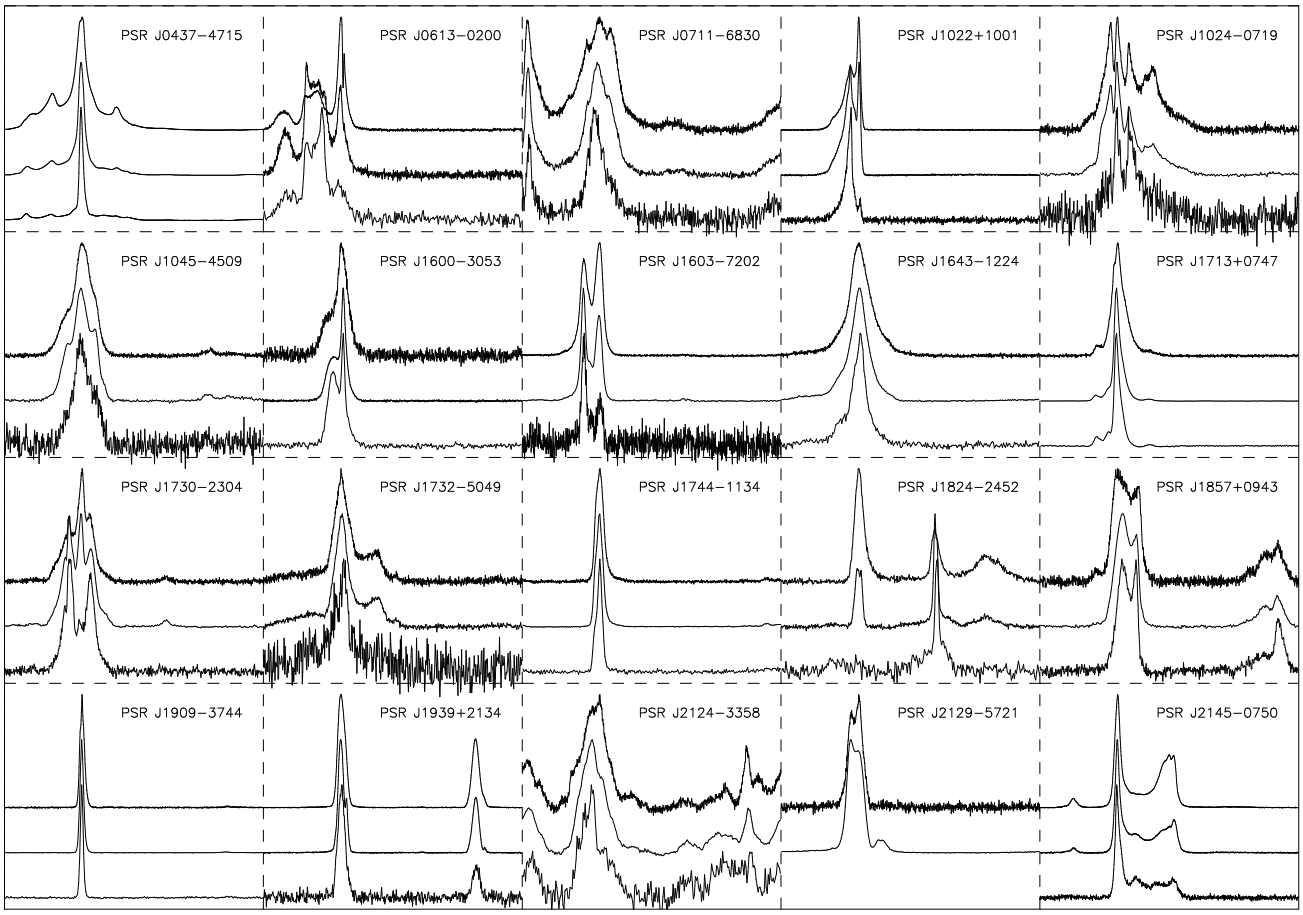

Figure 1. Stokes I profiles for the 20 millisecond pulsars in our sample. For each pulsar we give the 50 cm, 20 cm and 10 cm profiles from top to bottom respectively (except for PSR J2129−5721 where only 50 cm and 20 cm profiles are available).

roughly equal logarithmic sampling. Estimation of $D_{\rm DM}(\tau)$ for a power-law process from a single "realisation" of the process incurs a significant error which has been discussed by Rickett et al. (2000). For Kolmogorov processes they found that the estimation error $\sigma_{\rm est}(\tau) \propto D(\tau)[\tau/(T-\tau)]^{1/3}$ where T represents the data-span. We have extended their simulations to pure power-law processes which do not have a defined low frequency limit (or "outer scale"). For uniformly sampled data from a Kolmogorov process we find that

$$\sigma_{\rm est}(\tau) = 1.66 D(\tau)(\tau/T)^{1/3}. \quad (9)$$

Assuming that the process itself has Gaussian differences, the structure function estimator must be χ^2-distributed, and defined by $N_{\rm dof}$, the number of degrees of freedom. The estimation error can be written in terms of $N_{\rm dof}$ as $\sigma_{\rm est}(\tau) = D(\tau)(2/N_{\rm dof})^{0.5}$, so $N_{\rm dof} = 0.72(T/\tau)^{2/3}$. As our data are irregularly sampled we sometimes have fewer pairs, N_p, or fewer samples, N_s, contributing than $N_{\rm dof}$. We therefore approximate the actual number of degrees of freedom as the minimum of $(N_p, N_s, N_{\rm dof})$.

In addition to the estimation error discussed above, which is the amount by which a single realisation of a random process can be expected to depart from the theoretical mean, we must consider the fact that the measurements include a white noise component independent of DM(t). We assume that the errors on the ΔDM(t) values are independent, Gaussian and have known, but different, standard deviations. These contribute a different bias and error to each $D_{\rm est}(\tau)$ which are computed by expanding each $D_{\rm est}(\tau)$ as shown in Appendix A.

Our work contrasts with earlier estimates of the structure function. In earlier work, the uncertainty on the structure function was either estimated as the standard deviation divided by the square root of the number of points (Cordes et al. 1990) or as the smaller of the number of points and (T/τ) (Ramachandran et al. 2006). The choice of the bias term which is subtracted from $D_{\rm DM}(\tau)$ has also been inconsistent in the literature. Usually the bias has been taken as the average of the ΔDM(t) errors. This method is only accurate when the number of points is very large and the error on ΔDM(t) is significantly smaller than its value. Earlier work also did not allow for the error on the measured ΔDM(t) values which, for some data-sets, is very important.

It is useful to obtain the diffractive time-scale, τ_d, and bandwidth, ν_d, for each pulsar to compare with the $D_{\rm DM}(\tau)$. For many pulsars we were able to obtain these values from the literature. Table 2 gives these τ_d and ν_d values. In column order, the Table contains the pulsar name, observing frequency, τ_d, ν_d and a bibliographic reference. However, no measurements existed for nine of our pulsars. As our data have relatively poor frequency and time resolution (for this purpose), we obtained τ_d and ν_d using a structure function analysis (Rickett et al. 2000) rather than the more standard method of using the auto-correlation function of the dy-

Table 2. Scintillation parameters for the PPTA millisecond pulsars

PSR Name	Freq. (MHz)	τ_d (min)	ν_d (MHz)	Ref.
J0437−4715	327	1.9 – 5.1	0.18 – 3.0	1
	436	4.6 – 11	3.2 – 4.4	2,3
	660	7.8	17	2
J0711−6830	436	13	0.37	2
	660	16	1.2	2
J1600−3053	1373	4.7	< 0.5	4
J1603−7202	660	9.2	0.36	2
J1713+0747	430	14	0.6	5
	436	28	1.5	2
J1730−2304	327	7.4 – 7.5	0.10 – 0.12	1
	436	6.3 – 12	0.15 – 0.18	2,3
	660	9.7	1.4	2
	1520	23-27	30 – 38	2,3
J1744−1134	436	21	1.3	2
	660	20	2.3	2
J1939+2134	320	1.1	0.0014	6
	430	1.7	0.0042	6
	1400	7.4	0.92	6
J2124−3358	436	44	6.9	2
J2129−5718	436	11	0.29	2
	660	17	1.3	2
	1520	24	58	2
J2145−0750	327	6.4	0.33	1
	436	21-25	0.61 – 2.5	2,3

Reference: (1) Gothoskar & Gupta (2000); (2) Johnston et al. (1998); (3) Nicastro & Johnston (1995); (4) Ord et al. (2006); (5) Bogdanov et al. (2002); (6) Cordes et al. (1990).

namic spectrum. The implementation of this technique is discussed in Appendix B. From each τ_d measurement we have used the definition that $D_\phi(\tau_d) = 1$ to obtain an estimate of

$$D_{\rm DM}(\tau_d) = (K\nu/2\pi)^2. \quad (10)$$

4 RESULTS

The variation of DM with time, $\Delta{\rm DM}(t)$, for each pulsar is shown in Figure 2. We list, in Table 3, the bands used for each pulsar and the interval over which the $\Delta{\rm DM}(t)$ values were measured and the slope of the best-fitting straight line d${\rm DM}/{\rm d}t$. The panels in Figure 2 are chosen so that all pulsars have the same time axis, but different scalings are used for the ordinate. We see large-scale DM variations for six of our pulsars (PSRs J0437−4715, J1045−4509, J1643−1224, J1824−2452, J1909−3744, J1939+2134) with a maximum range in $\Delta{\rm DM}$ of $\sim 0.014\,{\rm cm}^{-3}\,{\rm pc}$ for PSR J1045−4509.

4.1 Diffractive scintillation parameters

Using the method described in §3, we obtained diffractive scintillation timescales for 17 of our pulsars, obtaining τ_d and ν_d values for each observation with a high S/N. In column order, Table 4 contains the pulsar name, observing frequency and the range of our measured τ_d and ν_d values, respectively. For pulsars where previous measurements exist

Table 3. Summary of the DM variations for the PPTA pulsars

PSR Name	Band (cm)	Interval (d)	d${\rm DM}/{\rm d}t$ (${\rm cm}^{-3}$ pc ${\rm yr}^{-1}$)	Data Span (yr)
J0437−4715	10, 50	15	$1.0(2) \times 10^{-5}$	3.0
J0613−0200	20, 50	15	$-9(2) \times 10^{-5}$	2.9
J0711−6830	20, 50	15	$-2.5(9) \times 10^{-5}$	2.8
J1022+1001	10, 50	7	$-5(60) \times 10^{-6}$	2.7
J1024−0719	20, 50	15	$3.2(9) \times 10^{-4}$	2.9
J1045−4509	20, 50	15	$-5.56(9) \times 10^{-3}$	2.9
J1600−3053	10, 20	15	$-9(2) \times 10^{-4}$	2.7
J1603−7202	20, 50	15	$1.28(5) \times 10^{-3}$	2.6
J1643−1224	20, 50	15	$-1.18(6) \times 10^{-3}$	2.6
J1713+0747	20, 50	15	$5(23) \times 10^{-6}$	2.7
J1730−2304	20, 50	7	$3.9(8) \times 10^{-4}$	2.5
J1732−5049	20, 50	7	$-7(1) \times 10^{-4}$	2.4
J1744−1134	20, 50	15	$5(2) \times 10^{-5}$	2.7
J1824−2452	20, 50	12	$6.0(1) \times 10^{-3}$	1.1
J1857+0943	20, 50	15	$1.5(1) \times 10^{-3}$	2.2
J1909−3744	20, 50	15	$-3.28(6) \times 10^{-4}$	2.7
J1939+2134	20, 50	15	$2.57(2) \times 10^{-4}$	2.3
J2124−3358	20, 50	15	$2.5(8) \times 10^{-4}$	2.7
J2129−5721	20, 50	7	$-2(3) \times 10^{-4}$	0.9
J2145−0750	20, 50	15	$4.0(4) \times 10^{-4}$	2.4

our results are consistent with values in the literature. The scatter in τ_d observations is much greater than the error bars on individual τ_d measurements. We have confirmed, by simulation, that the reason for this is that τ_d is estimated from observations which are much shorter than the refractive scale.

For three pulsars it was difficult for us to obtain diffractive time-scale measurements. For PSR J0437−4715, this is not a problem as there are many measurements available in the literature. The diffractive time-scale for PSR J1824−2452 is too short at 20 cm (less than 1 min) for us to measure. At 10 cm, this pulsar is very weak (SNR ∼20 for a 1 hr observation), but we were able to obtain a few usable observations. The τ_d for PSR J2124−3358 is relatively long. From the $\tau_d = 44$ min at 436 MHz (Johnston et al. 1998), we can estimate that τ_d at 685 MHz is ∼76 min, but our current observation time for this pulsar is only 32 min.

4.2 Structure functions

We have calculated structure functions from $\Delta{\rm DM}(t)$ for each of our pulsars. Representative examples are shown in Figure 3 and Figure 4. In these figures, we have included τ_d measurements obtained from the literature (cross-symbols) or from our data (open triangle symbols). For some pulsars, we have been able to derive an estimate of $D_{\rm DM}$ at large time lags from d${\rm DM}/{\rm d}t$ measurements in the literature (Hobbs et al. 2004) that were obtained using a single dataset[4]; such points are indicated using a full square-symbol at the rightmost edge of the plot. To put the data in context, we have drawn two theoretical lines fitted through the τ_d points,

[4] A given d${\rm DM}/{\rm d}t$ measurement can be converted to a single point on a structure function as $({\rm dDM}/{\rm d}t \cdot T)^2$, where T is the data span.

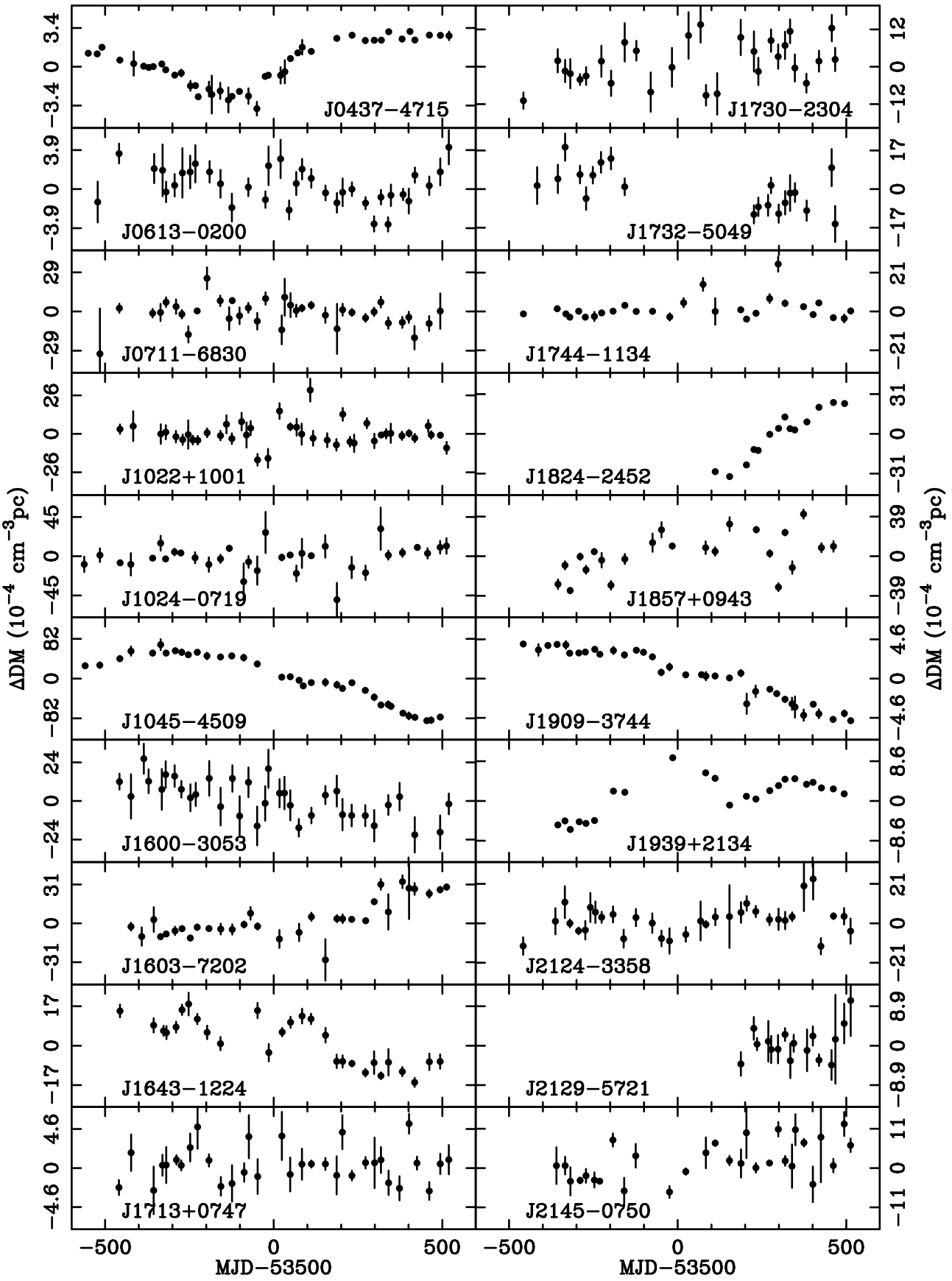

Figure 2. DM variations of 20 millisecond pulsars. Note a ΔDM of 10^{-4}cm^{-3}pc corresponds to time delays at 10 cm of 43 ns, at 20 cm of 212 ns and at 50 cm of 884 ns.

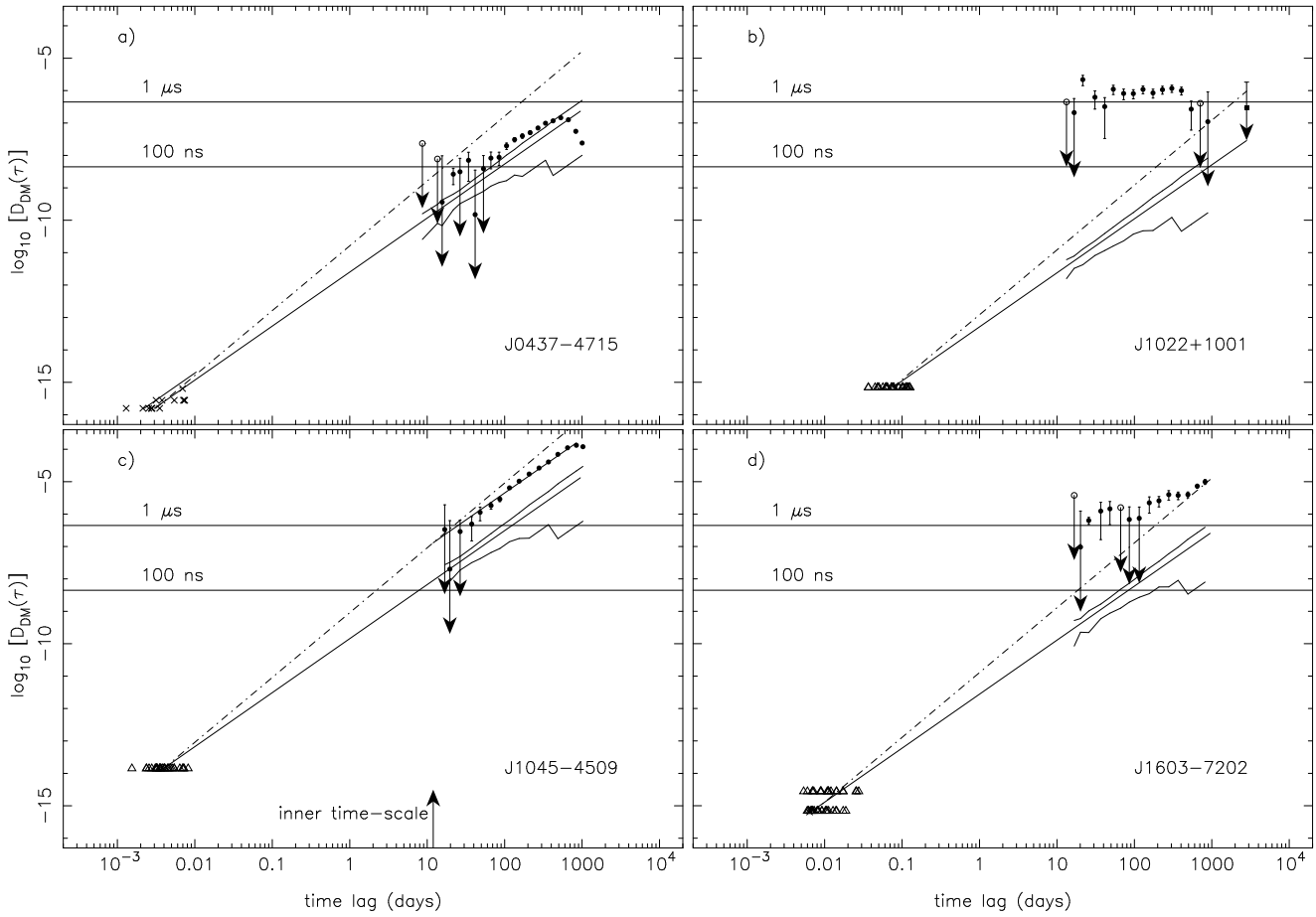

Figure 3. Structure functions, $D_{\rm DM}(\tau)$ for four pulsars. The τ_d derived estimates are marked by triangles from our data and crosses from the literature. The estimates obtained directly from the time series $\Delta{\rm DM}(t)$ as discussed in Appendix A are marked as filled circles with error bars. Open circles indicate a negative estimate. A Kolmogorov model fit to τ_d is shown using a solid line and a quadratic model is shown dash-dotted. Confidence limits on the Kolmogorov model are solid lines bracketting the model. Equivalent delays at 1400 MHz are shown for 100 ns and 1 μs. For PSR J1022+1001, a point derived from d${\rm DM}/{\rm d}t$ is shown as a solid box with error bars at the longest time lag.

one (full line) with the Kolmogorov exponent ($\alpha = 5/3$), the other (dashed-dotted line) with $\alpha = 2$ corresponding to the steepest possible structure function resulting from plasma turbulence (Rickett 1990) (hereafter, this spectrum is known as "quadratic"). Estimation error bounds on the theoretical Kolmogorov model (at the 68% confidence level) for each data point are plotted using solid lines that bracket the theoretical model.

The remaining symbols used on the figures are as follows. The structure function values measured from $\Delta{\rm DM}(t)$ are plotted using solid circle symbols. The errors on these points are estimated from the uncertainty on $\Delta{\rm DM}(t)$. For cases where the error is larger than the value we use downward pointing arrow symbols for the lower bound on the error bar. As we subtracted the bias due to the uncertainties on the $\Delta{\rm DM}(t)$ measurements, it is possible for large uncertainties on $\Delta{\rm DM}(t)$ that the structure function values are negative. We indicate such points using open circles and a downward arrow plotted at $D_{\rm DM}(\tau)$ plus twice its error. The structure function plots all have the same scaling.

For comparison, we also indicate the value of $D_{\rm DM}$ that would be expected for white timing residuals with a given rms (σ_{rms}) at 1400 MHz. The relationship between the structure function of the timing residuals, $D_{\rm TOA}$, and the structure function of DM variations, $D_{\rm DM}$, is

$$D_{\rm DM} = D_{\rm TOA}(K\nu^2)^2. \quad (11)$$

If the timing residuals are white, then $D_{TOA} = 2\sigma^2_{rms}$. We indicate, using solid horizontal lines, white noise with an rms of 1 μs and 100 ns.

For PSRs J1045−4509, J1824−2452 and J1909−3744 we have added an indication of the inner time-scale (see §5.3). For PSRs J1939+2134 and J1824−2452, we also overlay a dotted line which is the structure function from earlier work (see §5.3).

Our τ_d values for PSR J0437−4715 can be compared with the work of Smirnova et al. (2006) who scaled the observations of Johnston et al. (1998) and Gothoskar & Gupta (2000) by a large factor, assuming that the scintillation index was much smaller than unity, although the scintillation index was not reported by the original observers. Smirnova et al. (2006) deduced a phase structure function which is two orders of magnitude lower than ours in the vicinity of τ_d.

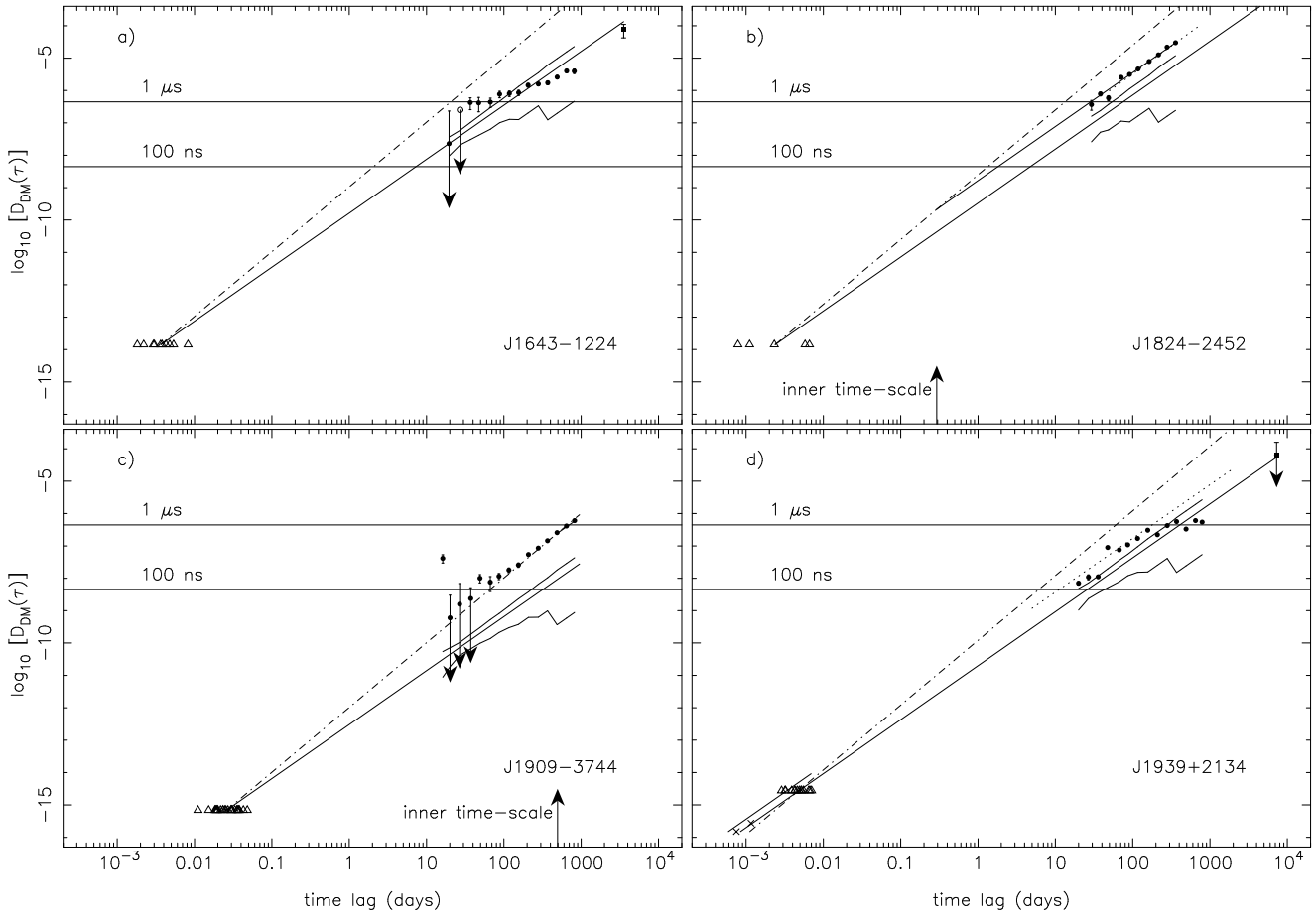

Figure 4. As for Figure 3, but for another four pulsars. For PSRs J1643−1224 and J1939+2134, a point derived from dDM/dt is shown as a solid box with error bars at the longest time lag.

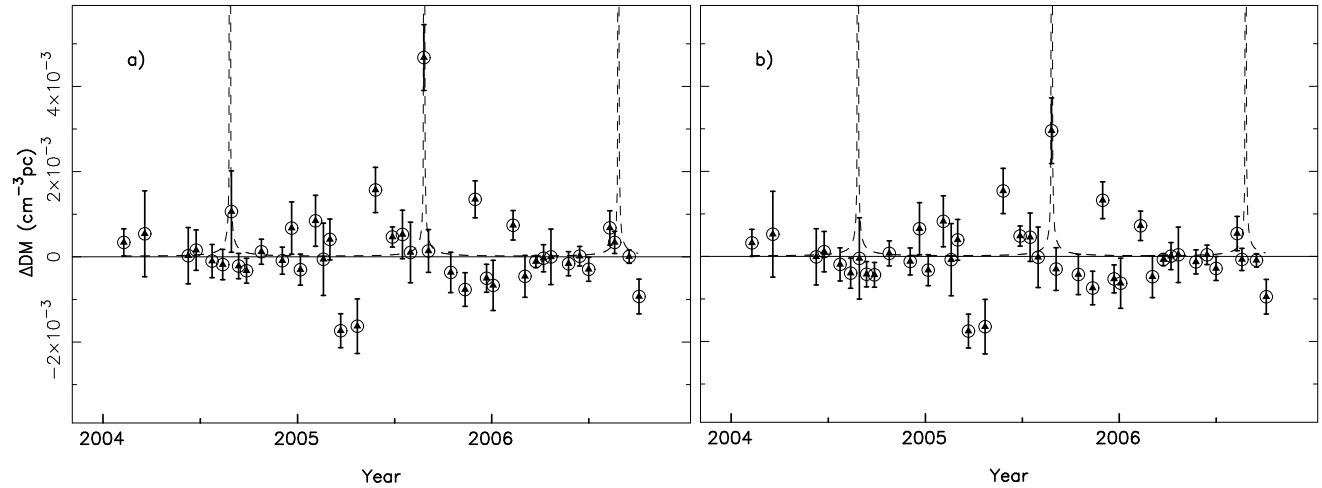

Figure 5. DM variations of PSR J1022+1001. The dashed curve is the TEMPO2 modelled $DM_\odot$ values. Panel a shows the DM variations with no correction for the solar wind. Panel b shows the DM variations after correction by the model used in TEMPO2.

4.3 Summary of results

For all the pulsars we find that the measured structure functions lie above the lower error bound of the Kolmogorov model. Two, PSRs J0437−4715 and J1939+2134, fit the Kolmogorov model well. Two, PSRs J1045−4509 and J1909−3744, are clearly inconsistent with a pure Kolmogorov power law, requiring a large inner scale. One, PSR J1824−2452, has few good τ_d measurements, but may well have $\tau_i > \tau_d$. The remaining 15 pulsars are dominated by white noise at small lags, and for five of these we can-

Table 4. Scintillation parameters from our observations

PSR Name	Freq. (MHz)	τ_d (min)	ν_d (MHz)
J0613−0200	1369	10 − 54	0.98 − 3.1
J0711−6830	685	18 − 42	1.0 − 5.4
	1369	36 − 127	30 − 77
J1022+1001	685	53 − 184	6.4 − 40
J1024−0719	685	23 − 89	4.8 − 47
J1045−4509	3100	2.2 − 12	0.64 − 15
J1600−3053	3100	4.0 − 23	1.90 − 6.9
J1603−7202	685	8.6 − 27	1.5 − 7.8
	1369	7.7 − 40	1.8 − 18
J1643−1224	3100	2.6 − 12	0.89 − 2.0
J1713+0747	685	20 − 47	1.8 − 11
J1730−2304	685	9.3 − 28	1.2 − 5.4
	1369	17 − 54	3.9 − 32
J1732−5049	1369	18 − 39	1.8 − 6.2
J1744−1134	685	29 − 76	4.1 − 40
J1824−2452	3100	1.1 − 9.5	0.6 − 1.1
J1857+0943	685	13 − 22	2.5 − 7.8
	1369	16 − 68	2.7 − 25
J1909−3744	685	16 − 69	2.8 − 20
J1939+2134	1369	4.1 − 10	1.8 − 5.4
J2129−5718	685	12 − 39	1.7 − 4.5
	1369	35 − 79	25 − 234
J2145−0750	685	20 − 111	2.9 − 44

not constrain the slope of the underlying power-law spectrum. Two pulsars (PSRs J1744−1134, J1857+0943) could not be classified on the basis of our measurements, but appear to be Kolmogorov on the basis of previously published dDM/dt values. For five pulsars (PSRs J0613−0200, J1600−3053, J1643−1224, J1713+0747 and J1732−5049) the structure functions fall below the quadratic model at large time lags, strongly suggesting that the underlying spectrum is Kolmogorov. The final three pulsars (PSRs J1603−7202, J1730−2304 and J2124−3358) appear to follow the quadratic model at large lags. However it should be realised that the structure functions at large lags are relatively poorly estimated and this separation of the pulsars into different categories is not perfectly clear.

The results described above lead us to propose that the structure functions for all our pulsars contain an ISM component that is either a pure Kolmogorov power-law or a Kolmogorov power-law with a large inner scale.

5 DISCUSSION OF DM MEASUREMENTS

5.1 Comparison with earlier work

Much of the earlier work has concentrated on measuring (and modelling) dDM/dt values (e.g. Backer et al. 1993; Hobbs et al. 2004). For comparison with earlier work we have listed in Table 3 the slope of the best-fitting straight line across the entire data-set for each of our pulsars, dDM/dt. Our values generally do not agree with the previously published values. However, for our data-sets, a single dDM/dt value models the observed $\Delta\mathrm{DM}(t)$ values well only for a few pulsars (PSRs J1045−4509, J1824−2452 and J1909−3744) and the dDM/dt values for other pulsars are misleading. For instance, for PSR J0437−4715 our results indicate that the DM evolution for this pulsar can roughly be described using three dDM/dt values: prior to MJD 53400 $\mathrm{dDM/d}t = (-2.98 \pm 0.07) \times 10^{-4}\mathrm{cm}^{-3}\mathrm{pc\,yr}^{-1}$, between MJD 53400 and 53700, $\mathrm{dDM/d}t = (6.2 \pm 0.2) \times 10^{-4}\mathrm{cm}^{-3}\mathrm{pc\,yr}^{-1}$ and subsequently $\mathrm{dDM/d}t = (3 \pm 1) \times 10^{-5}\mathrm{cm}^{-3}\mathrm{pc\,yr}^{-1}$. Clearly, the $\Delta\mathrm{DM}(t)$ values are better described using the structure function.

5.2 The solar wind

The solar wind leads to a significant change in DM for pulsars close to the ecliptic plane during close approaches of the line of sight to the pulsar with the Sun. According to the TEMPO2 model described in §2, an unmodelled solar wind contributes ∼100 ns at 1400 MHz for sources within 60° of the Sun and ∼1 μs within 7°. It is therefore clear that corrections are necessary for 18 out of our 20 PPTA pulsars. The correction can potentially be made by modelling the solar wind or by directly measuring the DM to sufficient accuracy using multiple frequency observations.

The solar wind varies with time and position. An overview of the relevant solar physics can be found in Schwenn (2006). Most of the variations in the solar wind are ascribed to a slowly changing spatial pattern that rotates with a 27-day period. In addition global transients, called coronal mass ejections (CME), occur every few days. The chances of a given observation, which typically has a duration of 30-60 min, encountering a CME are only a few percent, so these are not the most important effects. The quasi-static spatial pattern is roughly bimodal, the "slow solar wind" with high electron density is concentrated within about ±20° (McComas et al. 2000) and the "fast solar wind" with lower electron densities at higher latitudes. The density difference is a factor of four at 1 AU and increases near the Sun. The correction necessary for a given observation can then vary by a factor of four depending on how much of the line of sight is in the slow versus the fast wind.

Corrections for the solar wind have been attempted in both TEMPO and TEMPO2. Both programs implement constant-density spherically symmetric models. TEMPO uses a high density model where the electron density at 1 AU, $n_e(1\mathrm{AU}) = 10\,\mathrm{cm}^{-3}$, whereas TEMPO2 has a lower density model of $n_e(1\mathrm{AU}) = 4\,\mathrm{cm}^{-3}$. Splaver et al. (2005) and Lommen et al. (2006) used an identical spherically symmetric model, but fitted for the electron density. They obtained $n_e(1\mathrm{AU}) = 5 \pm 4\,\mathrm{cm}^{-3}$ and $n_e(1\mathrm{AU}) = 6.9 \pm 2.1\,\mathrm{cm}^{-3}$ respectively. However, it is not possible for a spherically symmetric model to correct the average timing residual due to the large difference in density between the fast and slow winds. This is clearly demonstrated by our PSR J1022+1001 observations. The left panel in Figure 5 shows the DM variations of this pulsar without correcting for the solar wind and gives the correction from the TEMPO2 model as a dashed line. The right panel shows the DM variations after correction using the TEMPO2 model. During the year 2004, the TEMPO2 model did accurately correct the effect. The original TEMPO model which uses a larger electron density overcorrects these observations. The opposite occurs during 2005, when the TEMPO2 model under-corrects the observations whereas the original TEMPO models the solar wind well.

It is possible to use coronal measurements to improve our correction by estimating which parts of the line of sight are in the fast and which in the slow wind. This can be demonstrated with our PSR J1022+1001 data, but it is not yet clear whether using an updated model to correct the observations improves on simply measuring the excess DM using multi-frequency observations. This work will be reported in a future publication.

5.3 Spectrum of the ISM

All but six pulsars are consistent with a Kolmogorov fluctuation spectrum with an inner time-scale smaller than τ_d. The clearest examples are PSRs J0437−4715 and J1939+2134. The structure function for PSR J0437−4715 lies slightly above the upper bound of the Kolmogorov model fit to the τ_d data. However, if the τ_d data were divided by a factor of 1.35 they would be consistent. A line with this shift is shown in Figure 3a through the τ_d data. Given the large scatter in τ_d we consider that there is no evidence for an inner scale, nor do we see a need to rescale $D_\phi(\tau_d)$ as did Smirnova et al. (2006). The structure function at the largest time-scales is currently consistent with a Kolmogorov process, but there is an indication that the structure function may be flattening at these scales, as if an outer scale around 60 AU were present. We do not expect such a small outer scale, but it is not impossible if the turbulence has inhomogeneities of this order. Such structures could be caused, for example, by shear instabilities or due to a large-scale damping mechanism such as ion-neutral damping. The presence or absence of this flattening will become clearer in a few years, as we accumulate more observations of this pulsar.

There have been several analyses of the structure function for PSR J1939+2134 (Cordes et al. 1990; Ramachandran et al. 2006). The recent result of Ramachandran et al. (2006) is overlaid on our structure function in Figure 4d. They fitted for the power-law exponent and obtained $\alpha = 1.66 \pm 0.04$. They also compare their $D_{\rm DM}$ with a single τ_d measurement of 180 s. This comparison suggests an inner scale of 1.3×10^9 m. Our $D_{\rm DM}$ observations are slightly above the Kolmogorov model fit to the τ_d observations. However, as with PSR J0437−4715 there is a large scatter in τ_d. A shift of 1.43, shown as a solid line through the data in Figure 4d, would make the $D_{\rm DM}$ consistent. Thus we believe that the case for an inner time-scale greater than τ_d is weak for this pulsar.

The structure functions for PSRs J1045−4509 and J1909−3744 both lie well above the upper bound of the Kolmogorov spectrum and require an inner scale which is much larger than $V\tau_d$. We can identify a break in the structure function for PSR J1045−4509 which suggests an inner time-scale of about 12 d. The observations of PSR J1909−3744 can set a lower bound on the inner time-scale of 500 d. To our knowledge these are the first observations of such large inner scales. In order to estimate the corresponding spatial scales we use $V \approx 3.85 \times 10^4 (\nu_d D)^{1/2}/(\nu\tau_d)$ for a thin screen (Gupta et al. 1994). In both cases the inner scales of 0.7 and 20 AU are comparable to or larger than the refractive scales of 0.38 and 0.19 AU respectively [5]. These scales are so large that they can only be compared with ion-neutral damping scales. Ion-cyclotron damping at such scales would require absurdly low densities (see Equation 8).

Measurements of the structure function for PSR J1824−2452 have been published by Cognard & Lestrade (1997) and shown to be consistent with a Kolmogorov process. In Figure 4b we overlay the earlier structure function (dotted line) with our results. The two analyses are consistent. Our τ_d estimates suggest that $\tau_i > \tau_d$, but because there are few measurements of τ_d and the inferred τ_i is not as a large as for PSRs J1045−4509 and J1909−3744, the evidence for a large inner scale is weak.

In analysing the structure functions we have assumed that the line-of-sight velocity is constant. However the true velocity is a vector sum, weighted by the distance of the scattering plasma, of the pulsar proper motion, the orbital velocity for binary pulsars, the velocity of the plasma with respect to the local standard of rest and the orbital velocity of the earth (Rickett et al. 2000). For many of our pulsars these effects are important. Thirteen of our pulsars are in binary systems, and in five of those the orbital velocity is comparable with the proper motion. In all five of these plus another four non-binary pulsars the Earth's orbital velocity is also comparable. For these pulsars the magnitude and direction of the velocity can change significantly, both on a time-scale of days, and annually.

Diffractive observations are made on a time-scale which is short compared to the orbital periods, so such observations are affected by the instantaneous vector sum of velocities. DM variations are normally averaged over times longer than the typical binary periods in our sample, but shorter than a year. Thus these measurements are not affected by the binary orbital velocity. On average the diffractive observations see a higher velocity than the DM observations which will lead to the temporal structure function being flatter than the spatial structure function. If the turbulence in the interstellar plasma is anisotropic, and there is increasing evidence that such anisotropy is common, then the apparent diffractive time-scale will depend strongly on the direction of the velocity.

The net effect on our estimation of the structure function of DM is not large, because four of our five best constrained observations have relatively small velocity modulation. However, observations of the solitary pulsar PSR J1939+2134 are strongly modulated by the Earth's orbital velocity. In this case both diffractive and DM observations see the same time-varying velocity so the slope of the structure function is not altered, but both observations will be "noisier" than expected. In fact, the $D_{\rm DM}(\tau)$ for this pulsar is noisier than expected, suggesting that we are seeing the effect of annual variations in velocity. This effect is largest in PSR J2145−0750, for which the proper motion and orbital velocity are both similar to the Earth's orbital velocity. This pulsar shows a wider spread in τ_d than most. The structure function for this pulsar is white-noise dominated, making it difficult to estimate its slope of the

[5] The refractive time-scales are found using $t_r \approx 2\nu/\nu_d\tau_d$ (Rickett 1990)

structure function. The expected velocity modulation makes it even more difficult, so even though the structure function appears to be Kolmogorov on the basis of a single dDM/dt value, more observations are required to confirm this.

In PSRs J1045−4509 and J1909−3744 we observe intensity variations at the diffractive time-scale. However if the inner scales were greater than the refractive scales as they appear to be, then the structure function is quadratic and no intensity scintillation should be observed[6](Wandzura 1980). Thus there must be an underlying Kolmogorov process which is roughly equal in amplitude to the steep-spectrum process at τ_d.

This situation has been proposed theoretically (Zweibel, private communication 2006). It can arise when the primary energy input to the turbulence is at scales larger than the ion-neutral damping scale. Energy will cascade down to the ion-neutral scale where most of it will be absorbed. However some energy may 'tunnel' through the damping region to support a second Kolmogorov cascade at a lower level (in the vicinity of the ion-neutral collision frequency, plasma waves are evanescent).

In the case of PSR J1045−4509 the energy difference is about a factor of 30. For PSR J1909−3744 we can only say that the energy difference is at least a factor of 30. This is a very intriguing possibility which requires both observational and theoretical followup. The existence of steep spectra might be confirmed by VLBI observations which should show an rms position wander of $\lambda/(2\pi V\tau_d)$ on a time-scale of the inner time-scale (where λ is the wavelength). The baselines needed for a 1 rad rms phase difference are $V\tau_d$, where τ_d scales as $\nu^{1.2}$. This is about 8000 km for PSR J1045−4509 and 6000 km for PSR J1824−2452 at 1400 MHz. It would be much more difficult to measure PSR J1909−3744 as the baseline, even at 327 MHz, would be 50000 km and the time-scale for position wander would be greater than 500 d.

5.4 White noise

Twelve of our pulsars show a well-defined flattening of the structure functions at small lags which indicates the presence of a white-noise process that is substantially greater than the measurement error. Although this has not been discussed in the context of DM measurements before, it is a well-known anomaly in TOA measurements. Observers have often rescaled their measurement error estimates to match this white noise, but it is not clear that the additional white noise is due to measurement error. It could be due to a process intrinsic to the pulsar, unexplained calibration issues, or to diffractive TOA noise. The latter process will have the same time scale as diffractive intensity scintillation and is highly correlated with the intensity scintillation. Its rms is of the order of $\tau_0 = 1/(2\pi\nu_d)$. Although this phenomena has not been well-studied, it has been observed directly (Lestrade et al. 1998) and discussed theoretically (Romani et al. 1986). We have compared the observed white noise rms with τ_0 for each pulsar and find that this mechanism will need to be considered for four of the PPTA pulsars: PSRs J1045−4509, J1600−3053, J1643−1224 and J1939+2134. Since this mechanism is correlated with intensity it may be possible to use intensity measurements to correct it. It is likely that most of the white noise is related to system calibration errors as it is known, at least for some pulsars, to depend on the observing frequency and backend instruments.

[6] A pure quadratic structure function corresponds to a linear phase gradient, which simply shifts the apparent position of the source and does not change the intensity.

6 CORRECTION OF RESIDUALS FOR DM VARIATIONS

During the design of the PPTA project it was realised that DM variations would be an important source of timing noise and, unless corrected, would obscure the signature of many interesting phenomena such as gravitational waves. Initial expectations were that observations using the dual-band receiver would be used to determine $\Delta\mathrm{DM}(t)$ which, in turn, would be used to correct the 20 cm timing residuals. Of course, the measurements of DM include a white-noise component discussed earlier and hence, the correction for the "red" DM variations adds white noise. Smoothing the DM data before making the correction will reduce the white noise more than the DM noise. However, choosing the optimal smoothing is non-trivial.

The problem is that the timing model includes numerous terms such as parallax, position, proper motion, period and period derivative that absorb some of the residuals due to DM variations. Fitting the timing model to the residuals can substantially reduce the effect of DM variations, but causes significant errors in the fitted parameters. We cannot use the post-fit rms timing residual as a goodness measure, since it would not change at all after correction if the DM effect has been totally absorbed in the fitted parameters. Accordingly we have calculated the optimal smoothing factor using a simple analytical model which requires equally spaced observations. We have also simulated the observations at the actual sampling intervals with known model parameters and determined the optimal smoothing for the simulated data without having to fit a timing model. This work is outlined in Appendix C.

An example of the correction process is shown in Figure 6. We have shown the post-fit residuals for PSR J1939+2134 before correction (with an rms timing residual of 0.291 μs), and after correction (rms of 0.193 μs). We can assume that the timing model after correction is much more accurate than before correction. Therefore we have plotted the residuals of the uncorrected data using the more accurate corrected model resulting in an rms of 0.941 μs. The total proper motion, pulse-frequency, and frequency derivative were changed during the correction process by 7σ, 28σ and 28σ respectively.

Figure 6 shows clearly the necessity of correction for DM variations, and it also shows how fitting a timing model can spuriously remove a "red" process. For instance, if the TOA variations included the signature of a gravitational wave which resembled the DM variations (both are expected to have a steep, "red" signature) then fitting the timing model would also have removed most of the gravitational wave signature. Fortunately as the duration of the timing data increases it becomes harder for the timing model to emulate either the DM variations or the signature of gravitational

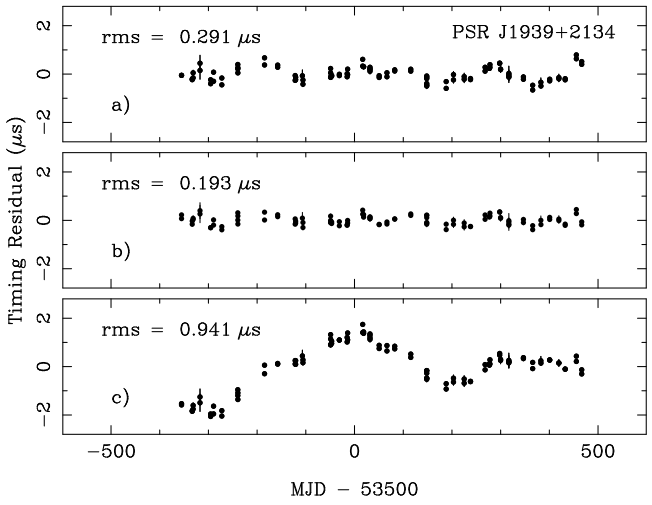

Figure 6. Timing residuals for PSR J1939+2134. The upper panel (a) shows the timing residuals before DM correction, panel (b) contains the timing residuals after correcting for the DM variations using a 71 day smoothing. Panel (c) shows the residuals obtained using the corrected parameters with the uncorrected TOAs.

waves. This is because the terms related to the motion of the Earth have annual or semiannual periods so they are not as effective at removing longer period variations.

The process described above has also been applied to five other pulsars for which DM fluctuations are important. For each of these pulsars, the theoretical smoothing time for uniformly sampled data and the actual optimal smoothing time from the simulation are given in the first two columns of Table 5. The rms timing residuals corresponding to the three panels of Figure 6, "original", "corrected", and "true uncorrected" (where the corrected pulsar parameters are used to model the uncorrected TOAs), are tabulated in the last three columns of the table. There is a correlation between the improvement of the residuals and the slope of $\Delta\mathrm{DM}(t)$. The pulsars with the least slope, PSRs J0437−4715 and J1939+2134, showed the most improvement in rms after correction for the DM variations. This is because a linear slope can be corrected exactly, but spuriously, in the original fitting. The $\Delta\mathrm{DM}(t)$ values for all except the last pulsar in the table are dominated by the plasma contribution. These all show significantly higher "true uncorrected" residuals demonstrating that the correction process was important even though it may not have significantly lowered the rms timing residuals. The last pulsar, PSR J1643−1224, is dominated by white noise and does not show much improvement in residual, nor is the true uncorrected residual much larger. As the PPTA continues to collect more data, the DM corrections will become increasingly important and will have to be applied to more of the observed pulsars.

7 CONCLUSIONS

We have shown that correction for the plasma delay is essential for the purposes of the PPTA project and have developed an optimal way of applying this correction.

We also show that the spherically symmetric solar wind models included in the pulsar timing packages TEMPO and TEMPO2 are of marginal value. More sophisticated models may be useful, especially in situations where it is difficult or impossible to measure the DM variations directly.

We have analysed the observed DM variations and found that most are consistent with a simple Kolmogorov model of interstellar turbulence with dissipation at a relatively small scale such as would be caused by ion cyclotron damping. However at least two of the 15 pulsars for which we can estimate the spectral exponent require a steeper spectrum and suggest strongly that ion-neutral collisions are important in damping the turbulence spectrum at AU scales.

Table 5. Improvement of timing residuals after correction for the DM variations.

PSR Name	T_{sm}^{theory} (d)	$T_{sm}^{simu.}$ (d)	σ_{orig} (μs)	$\sigma_{\mathrm{cor.}}$ (μs)	$\sigma_{\mathrm{uncor.}}$ (μs)
J1939+2134	100	71	0.291	0.193	0.941
J1824−2452	54	51	0.937	0.883	4.111
J0437−4715	243	91	0.396	0.316	0.509
J1909−3744	163	211	0.192	0.186	0.605
J1045−4509	116	201	3.862	3.800	9.386
J1643−1224	281	361	2.770	2.732	3.200

ACKNOWLEDGEMENTS

X. P. Y. is supported by the National Natural Science Foundation (NNSF) of China (10521001). The data presented in this paper were obtained as part of the Parkes Pulsar Timing Array project which is a collaboration between the ATNF, Swinburne University and The University of Texas, Brownsville. The Parkes radio telescope is part of the Australia Telescope which is funded by the Commonwealth of Australia for operation as a National Facility managed by CSIRO.

REFERENCES

Backer D. C., Hama S., Van Hook S., Foster R. S., 1993, ApJ, 404, 636
Bhat N. D. R., Cordes J. M., Camilo F., Nice D. J., Lorimer D. R., 2004, ApJ, 605, 759
Bogdanov S., Pruszunska M., Lewandowski W., Wolszczan A., 2002, ApJ, 581, 495
Britton M. C., van Straten W., Bailes M., Toscano M., Manchester R. N., 2000, in Kramer M., Wex N., Wielebinski R., eds, Pulsar Astronomy - 2000 and Beyond, IAU Colloquium 177. Astronomical Society of the Pacific, San Francisco, pp 73–76
Cognard I., Lestrade J.-F., 1997, A&A, 323, 211
Coles W. A., Harmon J. K., 1989, ApJ, 337, 1023
Coles W. A., Liu W., Harmon J. K., Martin C. L., 1991, J. Geophys. Res., 96, 1745
Cordes J. M., Lazio T. J. W., 2002, astro-ph/0207156
Cordes J. M., Wolszczan A., Dewey R. J., Blaskiewicz M., Stinebring D. R., 1990, ApJ, 349, 245
Edwards R. T., Hobbs G. B., Manchester R. N., 2006, MNRAS, 372, 1549

Freire P. C., Camilo F., Kramer M., Lorimer D. R., Lyne A. G., Manchester R. N., D'Amico N., 2003, MNRAS, 340, 1359
Gothoskar P., Gupta Y., 2000, ApJ, 531, 345
Gupta Y., Rickett B. J., Lyne A. G., 1994, MNRAS, 269, 1035
Hamilton P. A., Hall P. J., Costa M. E., 1985, MNRAS, 214, 5P
Hobbs G., 2005, PASA, 22, 179
Hobbs G., Lyne A. G., Kramer M., Martin C. E., Jordan C., 2004, MNRAS, 353, 1311
Hobbs G. B., Edwards R. T., Manchester R. N., 2006, MNRAS, 369, 655
Hotan A. W., van Straten W., Manchester R. N., 2004, PASA, 21, 302
Jenet F. A., Hobbs G. B., Lee K. J., Manchester R. N., 2005, ApJ, 625, L123
Johnston S., Nicastro L., Koribalski B., 1998, MNRAS, 297, 108
Kaspi V. M., Taylor J. H., Ryba M., 1994, ApJ, 428, 713
Lestrade J., Rickett B. J., I. C., 1998, A&A, 334, 1068
Lommen A. N., Kipphorn R. A., Nice D. J., Splaver E. M., Stairs I. H., Backer D. C., 2006, ApJ, 642, 1012
Lyne A. G., Pritchard R. S., Smith F. G., 1988, MNRAS, 233, 667
Manchester R., 2006, astro-ph/0604288
Manchester R. N., Hobbs G. B., Teoh A., Hobbs M., 2005, AJ, 129, 1993
McComas D. J., Barraclough B. L., Funsten Gosling J. T., Santiago-Muñoz E., Skoug R. M., Goldstein B. E., Neugebauer M., Riley P., Balogh A., 2000, J. Geophys. Res., 105, 10419
Minter A. H., Spangler S. R., 1997, ApJ, 485, 182
Nicastro L., Johnston S., 1995, MNRAS, 273, 122
Ord S. M., Jacoby B. A., Hotan A. W., Bailes M., 2006, MNRAS, 371, 337
Phillips J. A., Wolszczan A., 1991, ApJ, 382, L27
Ramachandran R., Demorest P., Backer D. C., Cognard I., Lommen A., 2006, ApJ, 645, 303
Rickett B. J., 1977, Ann. Rev. Astr. Ap., 15, 479
Rickett B. J., 1988, in Cordes J., Rickett B. J., Backer D. C., eds, Radio Wave Scattering in the Interstellar Medium, AIP Conference Proceedings 174 American Institute of Physics, New York, pp 2–16
Rickett B. J., 1990, Ann. Rev. Astr. Ap., 28, 561
Rickett B. J., Coles W. A., Markkanen J., 2000, ApJ, 533, 304
Romani R. W., Narayan R., Blandford R., 1986, MNRAS, 220, 19
Schwenn R., 2006, Living Reviews in Solar Physics, 3, 2
Smirnova T. V., Gwinn C. R., Shishov V. I., 2006, A&A, 453, 601
Splaver E. M., Nice D. J., Stairs I. H., Lommen A. N., Backer D. C., 2005, ApJ, 620, 405
Wandzura S. M., 1980, Journal of the Optical Society of America (1917-1983), 70, 745
Wang N., Johnston S., Manchester R. N., 2004, MNRAS, 351, 599

APPENDIX A: CALCULATION OF THE STRUCTURE FUNCTION

Let $D_{\rm est}(\tau)$ be the estimated structure function for the DM variations at time lag τ. As described in §2, we assume that the errors on the $\Delta{\rm DM}(t)$ values are independent, Gaussian and have known, but different, standard deviations. The bias and error that these errors contribute to $D_{\rm est}(\tau)$ are obtained by expanding each $D_{\rm est}(\tau)$ as

$$\begin{aligned} D_{\rm est}(\tau) &= \frac{1}{N_p}\left\{\sum_{ij}[\Delta{\rm DM}(i)-\Delta{\rm DM}(j)]^2\right. \\ &+ \sum_{ij}[e(i)^2+e(j)^2] \\ &+ 2\sum_{ij}[e(i)-e(j)][\Delta{\rm DM}(i)-\Delta{\rm DM}(j)] \\ &- \left. 2\sum_{ij}e(i)e(j)\right\}, \end{aligned} \tag{A1}$$

where N_p is the number of pairs, $\Delta{\rm DM}(i)$ is the ΔDM within the time lag "bin" τ , and $e(i)$ is the corresponding error. The first term in this expansion is the desired estimator and the other terms are uncorrelated errors. The second term is the only error term that does not have zero mean and so contributes a bias which must be calculated and subtracted from $D_{\rm DM}(\tau)$. The variances of each term are easily calculated and summed to give the total variance in $D_{\rm DM}(\tau)$. So finally, the calculated $D_{\rm DM}(\tau)$ is

$$\begin{aligned} D_{\rm DM}(\tau) &= \frac{1}{N_p}\left\{\sum_{ij}[\Delta{\rm DM}(i)-\Delta{\rm DM}(j)]^2\right. \\ &- \left.\sum_i N_i\epsilon(i)^2\right\} \end{aligned} \tag{A2}$$

where $\epsilon(i)$ is the rms of the $e(i)$, N_i is the number of times that $\Delta{\rm DM}(i)$ is used to calculate the $D_{\rm DM}(\tau)$. The variance of the $D_{\rm DM}(\tau)$ is

$$\begin{aligned} \sigma^2_{D_{\rm DM}}(\tau) &= \frac{1}{N_p^2}\left\{2\sum_i N_i^2\epsilon(i)^4\right. \\ &+ 4\sum_i\sum_j\epsilon(i)^2[\Delta{\rm DM}(i)-\Delta{\rm DM}(j)]^2 \\ &+ \left. 4\sum_{ij}\epsilon(i)^2\epsilon(j)^2\right\}. \end{aligned} \tag{A3}$$

We have developed a TEMPO2 plug-in that is publicly available (download and usage instructions are given in Appendix D) to carry out these calculations.

APPENDIX B: CALCULATION OF THE DIFFRACTIVE TIME-SCALE AND BANDWIDTH

The structure function of DM variations can be related to the diffractive time (τ_d) using Equation 5. Normally, the parameters of diffractive interstellar scintillation (time-scale τ_d and decorrelation frequency scale ν_d) are obtained using

a two dimensional auto-correlation function (ACF) of the dynamic spectrum $S(\nu, t)$ as

$$C(\Delta\nu, \Delta t) = \frac{1}{N_p(\Delta\nu, \Delta t)} \sum_{\nu} \sum_{t} \Delta S(\nu, t) \Delta S(\nu + \Delta\nu, t + \Delta t) \quad \text{(B1)}$$

where N_p is the number of pairs. $\Delta S(\nu, t) = S(\nu, t) - \bar{S}$ where $S(\nu, t)$ is the flux density and $\bar{S}$ is the mean flux density for the whole observation. The diffractive parameters are defined by $C(0, \tau_d) = C(0, 0)/e$ and $C(\nu_d, 0) = C(0, 0)/2$. The parameters τ_d and ν_d are obtained by fitting a 2 dimensional Gaussian to $C(\Delta\nu, \Delta t)$. However we often have an observed dynamic spectrum which is not much longer than τ_d and wider than ν_d.

We use a method based on the structure function instead of auto-correlation function to estimate the diffractive time-scale. In our data, the ACF is biased because we have few scintles in the dynamic spectra. For such cases the structure function, defined as $D(\Delta t) = [S(t) - S(t + \Delta t)]^2/N_p$, is a better estimator because it does not require estimation of $\bar{S}$. If $C(\Delta t)$ exists, then $D(\Delta t) = 2[C(0) - C(\Delta t)]$. We estimate $D(\Delta t)$ as

$$\widetilde{D}(\Delta t) = \frac{1}{N_p(\Delta t)} \sum_{\nu} \sum_{t} \left[\Delta S(\nu, t) - \Delta S(\nu, t + \Delta t)\right]^2. \quad \text{(B2)}$$

Because there is receiver noise which is white, the measured structure function is

$$D_m(\Delta t) = D(\Delta t) + D_w = 2C(0) - 2C(\Delta t) + D_w(\Delta t) \quad \text{(B3)}$$

where D_w is the structure function for the white noise.

$$\begin{aligned} D_w(\Delta t) &= 2\sigma^2 (\Delta t > 0) \\ &= 0 (\Delta t = 0) \end{aligned} \quad \text{(B4)}$$

where σ is the standard deviation of $S(\nu, t)$ measured over the entire data-span.

If we normalise the flux density, then $\bar{S} = 1$. For our observations, the diffractive scintillation is strong and the observing time is much less than the refractive time-scale, so $C(0) = 1$. From the Kolmogorov spectrum, $C(\Delta t) = \exp(-(\Delta t/\tau_d)^{5/3})$.

So finally we can write the measured structure function as

$$D_m(\Delta t) = 2[1 - \exp(-(\Delta t/\tau_d)^{5/3})] + D_w(\Delta t) \quad \text{(B5)}$$

The uncertainty $\sigma_{D_m}(\Delta t)$ is estimated as $\sigma_{D_m}(\Delta t) = D_m(\Delta t)\sqrt{\Delta t/T_o}$, where T_o is the observation time. We choose the equal log time interval points to fit because when Δt is large, the points are not independent. Then we can fit the parameters τ_d and D_w in Equation B5 to obtain the diffractive time-scale τ_d.

A similar analysis can be used to obtain the diffractive bandwidth, ν_d. However, in contrast to the determination of τ_d, we do not know the form of $C(\Delta\nu)$ and, hence, it is not possible to fit for ν_d and $D_w(\Delta\nu)$. However, $D_w(\Delta\nu) = 2\sigma^2 \approx D_m(\Delta\nu_m)$, where $\Delta\nu_m$ is the minimum frequency lag (in our data, it is typically 0.5 MHz). $D_w(\Delta\nu)$ is the bias term which must be subtracted. This leads to the structure function being,

$$D_s(\Delta\nu) = D_m(\Delta\nu) - D_m(\Delta\nu_m) = 2C(0) - 2C(\Delta\nu). \quad \text{(B6)}$$

After normalisation ($C(0) = 1$) and according to the definition of ν_d ($C(\nu_d) = C(0)/2 = 1/2$), we can obtain ν_d when $D_s(\Delta\nu) = 1$.

APPENDIX C: CALCULATING THE OPTIMAL SMOOTHING TIME

Let t_{g1} and t_{g2} be idealised TOAs that are affected by neither noise nor DM variations. These TOAs correspond to frequencies ν_1 and ν_2 respectively where $\nu_1 > \nu_2$. Similarly, t_{g1o} and t_{g2o} are observed TOAs at these frequencies which have been affected by noise and DM variations. So the observed TOAs are given by

$$t_{gio} = t_{gi} + n_i(t) + \frac{\Delta\mathrm{DM}(t)}{K} \nu_i^{-2} \quad \text{(C1)}$$

where $n_i(t)$ is the noise at ν_i which is assumed to be white ($i = 1, 2$ for the two observations respectively). The measured estimate of DM(t) is therefore given by

$$\begin{aligned} \widetilde{\mathrm{DM}}(t) &= [t_{g2o}(t) - t_{g1o}(t)] \frac{K}{\nu_2^{-2} - \nu_1^{-2}} \\ &= (t_{g2} - t_{g1}) \frac{K}{\nu_2^{-2} - \nu_1^{-2}} + \Delta\mathrm{DM}(t) \\ &\quad + [n_2(t) - n_1(t)] \frac{K}{\nu_2^{-2} - \nu_1^{-2}}. \end{aligned} \quad \text{(C2)}$$

After correcting for the DM variations, by subtracting the corresponding time offsets from t_{g1o}, we obtain a set of corrected TOAs, $t_{g1c}(t)$, which are given by,

$$\begin{aligned} t_{g1c}(t) &= t_{g1o}(t) - \frac{\widetilde{\mathrm{DM}}(t)}{K} \nu_1^{-2} \\ &= t_{g1} a_1 - t_{g2} a_2 + n_1(t) a_1 - n_2(t) a_2 \end{aligned} \quad \text{(C3)}$$

where $a_1 = \nu_2^{-2}/(\nu_2^{-2} - \nu_1^{-2})$ and $a_2 = \nu_1^{-2}/(\nu_2^{-2} - \nu_1^{-2})$. Note that, since $a_1 - a_2 = 1$, contributions to the timing residuals which are frequency independent and thus the same in t_{g1} and t_{g2}, appear unchanged in t_{g1c}. This is an important property of the correction algorithm because interesting contributions such as the signature of gravitational waves, planets orbiting the pulsar, or ephemeris errors are unaltered by the correction.

Comparing Equations C1 and C3 we see that the variance of the white noise has increased from σ_{N1}^2 to $\sigma_{N1}^2 a_1^2 + \sigma_{N2}^2 a_2^2$ although the DM noise has been eliminated. We can improve the variance in t_{g1c} by smoothing $\widetilde{\mathrm{DM}}(t)$ before subtracting it from t_{g1o}, because smoothing reduces the white noise more than the DM(t) variations. The white variance in $\widetilde{\mathrm{DM}}(t)$ is reduced by the smoothing number N_s. It is hard to calculate the effect of smoothing DM(t) analytically, but we found numerically that the variance of equally sampled [DM(t) − smoothed(DM(t))] $\approx 0.5 D_{\mathrm{DM}}(T_{sm}/2\pi)$ where $T_{sm} = (N_s - 1)\tau_0$ and τ_0 is the sampling time (typically 15 d). However, the white noise in the smoothed $\widetilde{\mathrm{DM}}(t)$ is partially correlated with that in t_{g1o}, so we have finally the variance in t_{g1c}

$$\begin{aligned} \sigma_{1csm}^2 &= \sigma_{N1}^2 + \frac{(\sigma_{N1}^2 + \sigma_{N2}^2) a_2^2}{N_s} + \frac{2 a_2 \sigma_{N1}^2}{N_s} \\ &\quad + \frac{1}{2} \left(\frac{1}{k\nu_1^2}\right)^2 \left(\frac{N_s - 1}{2\pi}\right)^{\alpha} D_{\mathrm{DM}}(\tau_0). \end{aligned} \quad \text{(C4)}$$

We minimise this numerically. In fact, the data are not equally sampled so we first interpolate the raw data on to an equally spaced array before smoothing. To check the effect of re-sampling we compared the theory above with a simulation. We realised 50 samples of DM(t) from a population matching DM(τ) with the actual data sampling. Then we interpolated the simulated data onto an equally spaced array and found the N_s which best corrected for DM(t). In all cases the minimum is very broad so it makes little difference whether one uses the theoretical or simulated value of N_s. However, the simulation is easy to implement and will be correct even in the case of an unusual distribution of samples.

APPENDIX D: AVAILABLE SOFTWARE

The TEMPO2 software was designed to allow for easy addition of new features and functionality in the form of plug-ins to the main package. During this work we have produced the following new plug-in packages which are now available as part of the TEMPO2 distribution (full details are available from our web-site, `http://www.atnf.csiro.au/research/pulsar/tempo2`):

- CALCDM: this plug-in contains the algorithms described in this paper. This plug-in allows the user to calculate and plot ΔDM(t) and obtain the corresponding structure function.
- SF: calculates and plots the structure function of the timing residuals.
- SIMISM: allows data-sets to be simulated in order to study the effect of a Kolmogorov process on pulsar timing residuals.

The program DIFFTIME can be used to calculate τ_d and ν_d for most pulsar observations. This software is available as part of the PSRCHIVE software distribution (`http://psrchive.sourceforge.net`).

Software to simulate the effect of refraction on τ_d estimates is in the SIM 2.0 distribution from UCSD: `http://typhoon.ucsd.edu/~coles/sim2.0/sim2.0.html`.